Journal of King Saud University – Science 34 (2022) 101738

Contents lists available at ScienceDirect

Journal of King Saud University – Science

journal homepage: www.sciencedirect.com

Original article

$ZnO/La_2O_3/NiO$ based ternary heterostructure nano-photocatalyst: Preparation, characterization and its application for the degradation of methylene blue

J.P. Shubha [a,*], N.V. Sushma [a], S.F. Adil [b,*], Mujeeb Khan [b], Mohamed E. Assal [b], Mohammad Rafe Hatshan [b], Baji Shaik [c]

[a] Department of Chemistry, Don Bosco Institute of Technology, Mysore Road, Bangalore 560074, India
[b] Department of Chemistry, College of Science, King Saud University, P.O. Box 2455, Riyadh 11451, Saudi Arabia
[c] Department of Advanced Materials Engineering for Information and Electronics, Kyung Hee University, 1732 Deogyeong-daero, Giheung-gu, Yongin-si, Gyeonggi-do 446-701, Republic of Korea

ARTICLE INFO

Article history:
Received 16 August 2021
Revised 23 November 2021
Accepted 24 November 2021
Available online 29 November 2021

Keywords:
$ZnO/La_2O_3/NiO$
Heterostructure
Sunlight
Photocatalyst
Methylene blue
Dye degradation

ABSTRACT

ZnO based ternary heterostructure ZnO/(X wt%)La_2O_3/NiO (X = 1%, 3% and 5% of La_2O_3) nanoparticles were successfully synthesized employing waste curd as fuel by facile one-pot combustion procedure. The composition, morphology and structure of the fabricated heterostructures were characterized using various microscopic and spectroscopic instruments including using XRD, FTIR, UV–Visible, EDX, FESEM and HRTEM analysis. To evaluate the photo-catalytic degradation efficacy of the prepared ternary nanocomposite, textile dye methylene blue (MB) was selected as benchmark reaction under solar irradiation. The influence of several catalytic variables including light source, catalyst loading, photocatalyst dose, MB concentration, irradiation time, and pH value on the photo-degradation performance was systematically examined and the results were discussed. The results reveal that 3 wt% La_2O_3 doped ternary ZnO/NiO photocatalyst exhibits excellent performance towards the photocatalytic degradation of the studied dye. The ternary heterostructure i.e. ZnO/(3 wt%) La_2O_3/NiO exhibits superior MB degradation efficacy of 98% at 150 min under natural solar irradiation. The obtained observations conclude that the prepared nanocomposite exhibits pH dependent photo-catalytic efficacy, and for better results, concentrations of dye and photocatalysts have to be kept in a specific range. Moreover, different light sources have also been applied and their results are compared.

1. Introduction

Recently, the organic dye molecules and their waste-water products from fabric, leather, paper, plastic and petrochemical industries have been seriously polluting the aquatic life (Maruthupandy et al., 2020). Most of those dyes considered as main ecological pollutants and roughly 10–15% of the dyes have been generated in the wastewater which is a major source of ecological pollution (Koutavarapu et al., 2020). The wastewater comes from aforementioned industries contains dyes and pigments that are extremely deleterious for environment and have mutagenic and carcinogenic effects on aquatic organisms, surrounding lands, as well as on human beings causing serious ailments like cancer etc... Furthermore, most of these industrial dyes have highly stability against temperature, light, chemical compounds and microbial action (Pirkarami and Olya, 2017). Therefore, the inappropriate treating of noxious chemicals in textile wastewater also has serious effect on the both terrestrial and aquatic organisms, by negatively affecting the natural environment and causes long-term health problems (Dutta et al., 2014). Over the last one decade, various physicochemical and biological techniques have been carried out for the handling of wastewater came from fabric industries, however, most of these processes were found to be ineffective and expensive (Gonte and Balasubramanian, 2016). Nevertheless, these processes require expensive operation and recurring

* Corresponding authors.
E-mail addresses: shubhapranesh@gmail.com (J.P. Shubha), sfadil@ksu.edu.sa (S.F. Adil).

Peer review under responsibility of King Saud University.

ELSEVIER Production and hosting by Elsevier

https://doi.org/10.1016/j.jksus.2021.101738
1018-3647/

expenses, hence these techniques are not appropriate for small-scale industry. Therefore, cost-effective, efficacious and eco-friendly alternative techniques are needed to resolve the above-mentioned issues of degradation of dyes existents in effluents (Alharthi et al., 2020).

There are several methods for the degradation of dyes and pollutants from waste-water includes ozonation, coagulation, electrochemical degradation, aerobic and an-aerobic microbial decomposition, adsorption, precipitation and photocatalytic degradation (Shah et al., 2020; Azam et al., 2018). The advanced-oxidation-processes (AOPs), have been attracted a lot of attention over traditional processes and considered one of the best techniques for degradation of dyes and pollutants, which includes metal oxide based semiconductor photo-catalysts, owing to simple and rapid oxidation (Alharthi et al., 2020). This promising strategy involves degradation of noxious organic dye molecules via a mechanism of oxidation by generation of hydroxyl ($OH^{\cdot}$) free radicals because of the existence of photo-catalyst under the effect of light source which could be ultra violet, visible light or sunlight light irradiation. Semiconductor photo-catalysts are able to degrade organic dyes and pigments into environmentally friendly and harmless molecules, including carbon dioxide and water (Natarajan et al., 2018). Additionally, photo-catalysts have several merits such as not harmful, economic, consume lower energy, and can be readily recycled (Li et al., 2017). Ultimately, several semiconductor-based photo-catalysts are developed, particularly, oxide semiconductors are found to be effective for the photocatalytic degradation of hazardous organic pigments e.g., NiO (Chaudhary et al., 2018), CuO, ZnO (Tahir et al., 2013), TiO_2 (Zhang et al., 2018), and Fe_2O_3 (Tahir, 2020).

ZnO is considered as one of the most important semiconducting oxides, and attracted growing interest owing to its extraordinary properties for photo-decomposition of harmful organic dyes (López et al., 2019). Besides, it has enormous applications including solar cells, transistors, gas sensors, optical devices, and cancer therapy (Shah et al., 2020). ZnO has various advantageous merits like low cost, earth abundant, environmental-friendly, non-toxic, good photo-sensitivity, high chemical stability, thermally stable, and simple synthesis process (Feng et al., 2018). These features make ZnO an exemplary choice for photocatalyst. These properties make ZnO an excellent choice for photocatalyst. Although these advantageous features ZnO also experiences the drawbacks such as wide band-gap, the photoinduced electron-hole pairs reunion at a faster rate and consequently limits the use of ZnO (Hernández-Carrillo et al., 2018). It could be inhibiting the fast reunion of photo-generated charge carriers by decreasing the band gap of ZnO. Moreover, the light absorption range of ZnO is predicted to be expanded to the visible light so as to improve the photo-catalytic efficacy of ZnO. Recently, various techniques have employed to decrease the ZnO band-gap and increase the photo-catalytic performance, including noble metal doping ions, metal deposition, carrier load, non-metallic doping, and composite semiconductor (Tang et al., 2020; Zhao et al., 2017). Among these processes, the ZnO is supported with both metals and non-metals which leads to synthesis of heterojunctions with second semiconductor component. The synthesis of heterojunctions will provide opportunities to raise the separation performance of photoinduced charge carriers. In a recent years, a various ZnO-based binary and ternary heterojunctions have been synthesized like, binary ZnO/ZnS heterostructures, ternary $ZnO/Cu_2O/Si$ nanowire arrays, and ternary $ZnO–ZnS–Gd_2S_3$ nanostructural array and so on (Bharathi et al., 2019; Saravanakumar et al., 2016; Tahir, 2021).

The ZnO-based ternary heterojunctions offer considerable potential by encouraging the transfer of electrons attributed to the existence of multicomponent photo-systems and hence, enhances the photo-catalytic decomposition of organic dye molecules (Liu et al., 2014). The heterojunction based ZnO systems efficiently expand the life span of photo-generated charge carriers and improves absorption of light. A controlled synthesis of ternary heterojunctions is the necessity of the hour (Martínez-Vargas et al., 2019). The heterojunction based ZnO systems are synthesized through several chemical and physical techniques such as chemical vapour deposition (CVD), sol–gel, co-precipitation, microwave heating, solvothermal, and hydrothermal methods. These processes require high-tech instruments, high temperature and longer time of reaction conditions (Atla et al., 2018). Contrary to the aforementioned procedures, the solution combustion procedure is cost-effective, short time consuming, consumes less energy and needs low effort to carry out the process, additionally; it is easy to scale up the process. Eco-friendly materials can be used as starting material and could be efficiently applied in this process. These parameters which are highly useful persuaded in exploring the preparation of ZnO-based ternary heterojunctions using another photoactive metallic oxide and lanthanides (Wang et al., 2016; El-Barasi et al., 2020).

Nickel oxide (NiO) is also considered as one of the most essential oxide semiconductors, which has been widely employed in photocatalytic applications. It can be enhancing the efficiency of photocatalytic system for generation of electron-hole pairs and improve the photo-decomposition kinetics by doping with ZnO attributed to the variation in energy of the band gap (Senobari and Nezamzadeh-Ejhieh, 2018). The NiO–ZnO based composite is considered as the most significant photo-catalytic protocols, which has received a considerable interest. Several reported studies stated that the enhancement of properties and efficacy of these materials by doping them with other metal oxides (Pirmoradi et al., 2017).

In this investigation, an attempt is made to prepare an eco-friendly and low cost ternary ZnO/(3 wt%)La_2O_3/NiO heterostructure through a facile one-step combustion process to achieve higher photo-degradation efficacy using MB dye as organic pollutant model as displayed in Scheme 1. The synthesized ternary ZnO/(X wt%)La_2O_3/NiO nanocomposites are employed as photocatalyst for decomposition and removal of MB under natural sunlight irradiation. The ternary heterostructure exhibits an enhanced photocatalytic performance. Notably, this is the first study on the preparation and evaluation of photo-catalytic efficiency of ternary ZnO/(X wt%)La_2O_3/NiO nanocomposite. The photo-catalytic observations illustrate that the ZnO/(3 wt%)La_2O_3/NiO nanocomposite show superior photo-catalytic efficacy for the MB degradation under sunlight irradiation than a dark and UV irradiation, and approximately 98% of MB is degraded in 150 min under the optimal conditions. This study offers new insights in fabrication of multicomponent ZnO-based photo-catalysts for environmental remediation.

2. Experimental section

2.1. Materials

With no further purification raw materials of analytical grades such as $Zn(NO_3)_2{\cdot}6H_2O$, $Ni(CH_3CO_2)_2{\cdot}4H_2O$, and $La(NO_3)_3{\cdot}6H_2O$ are employed. To make a model waste water sample containing MB dye (SD fine chemicals) solution is synthesized with distilled water (DW). Glass wares of BOROSIL make are utilized throughout the study.

2.2. Synthesis of ZnO/(X wt%)La_2O_3/NiO heterostructure

Equal volume of 0.1 M solutions of $Zn(NO_3)_2{\cdot}6H_2O$ and $Ni(CH_3CO_2)_2{\cdot}4H_2O$ is taken in beaker, while varying the volume of 0.1 M

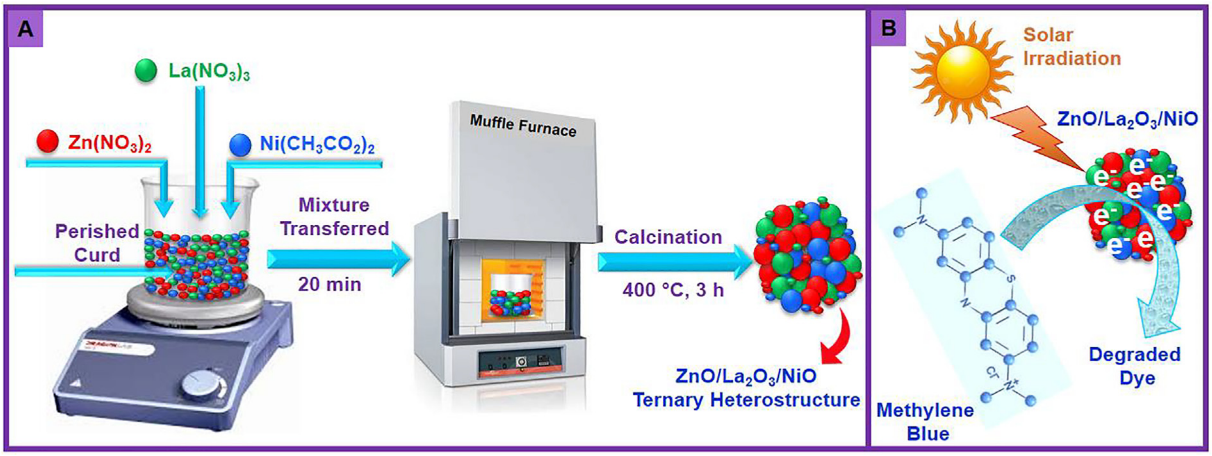

Scheme 1. (A) Scheme depiction of the fabrication of ternary heterostructure $ZnO/La_2O_3/NiO$ nanocomposite and (B) Scheme presentation the photo-degradation of MB dye.

solution $La(NO_3)_3{\cdot}6H_2O$ is added to obtain varying wt% of La_2O_3 in the terenary system, which is dissolved in 10 cm^3 of DW and optimized amount of perished curd i.e. 6 cm^3 is added to the solution with stirring for approximately 20 min. Thereafter, resultant sample is calcined in the muffle furnace at 400 °C. After 10 min a blackish green powder is obtained and which is further annealed at the identical temperature for 3 h.

2.3. Characterizations

The prepared photocatalysts have characterized by employing several common analysis and all specifics about instruments are included in supplementary file.

2.4. Photo-catalytic efficiency measurements

Theory of semiconductor-based photocatalysis states that the surface area, band gap, morphology, crystallinity, particle size, and amount of $OH^{\cdot}$ free radical on the surface of photo-catalyst determine its photo-catalytic efficacy (Zhang et al., 2018). The theory elucidates the releasing of electrons and holes on semiconductor surface by the absorption of light and the produced electrons and holes will participate in the reaction or they do reunion. If additional surface is provided for the electrons and holes, they will relocate where the electrons are caught by semiconductor while the holes are trapped by hydroxyl ions and produce $OH^{\cdot}$ and HO_2. For ternary structure, more surface is available for relocation of photogenerated charge carriers and therefore the produced hydroxyl ions are utilized efficiently to decompose MB dye. As per the obtained results from the UV–Vis spectroscopy, it is obvious that the synthesized heterostructures are active in the UV–Vis domain and the visible domain. Furthermore, the band gap calculated to be E_g = 3.79 eV. To assess the photocatalytic efficiency of the synthesized heterostructure i.e. $ZnO/(X\ wt\%)La_2O_3/NiO$, several parameters such as effect of light source, catalyst loading, photocatalyst dose, MB concentration, irradiation time and pH value are systematically studied and methylene blue is selected as the standard pollutant for photocatalytic decomposition in the investigation, and the variation of absorption peak intensity recorded at 663 nm (λ_{max} of MB) is monitored to conclude the obtained results.

For the present test, 100 cm^3 of aqueous solution of changing concentrations of MB dye such as 2.0, 5.0, 10.0 and 15.0 ppm are taken for photo-decomposition processes. The dosage of as-synthesized heterostructure is also varied 5, 10, 15, and 20 mg of $ZnO/(X\ wt\%)La_2O_3/NiO$. The solution is mixed with mixed metal oxide and aerated for 40 min, while kept in the dark. The kinetics of the degradation is examined by periodically collecting 3 cm^3 of aqueous mixture as sample from the solution at times of 30 min, which is then subjected to centrifugation. From the absorbance spectra obtained by using UV–Vis spectroscopy, the initial (C_0) and final (C_t) dye concentrations in the system is confirmed and the calculation for the degradation efficacy is done utilizing Eq. (1):

$$\text{Degradation efficiency} = \frac{(C_0 - C_t)}{C_0} \times 100 \quad (1)$$

3. Results and discussion

3.1. Characterization of the ZnO/(X wt%)La$_2$O$_3$/NiO heterostructures

The prepared samples are subjected to various characterization by various spectroscopic techniques. Fig. S1 displays the UV–Vis. absorption spectrum of the $ZnO/(3\ wt\%)La_2O_3/NiO$ heterostructure. The prepared sample exhibits the absorption in the range of (800–200 nm) with maximal absorption at approximately 242 nm along with an absorption edge from 390 to 405 nm, this indicates that the synthesized material is photolytically active in the UV domain as well as in the visible domain, furthermore it also shows the crystalline nature of the synthesized samples (Shubha et al., 2021; He et al., 2005). The band-gap of the prepared photocatalyst is found to be 3.69 eV which is calculated from Kulbeka-Munk equation. Broad range of absorption of light assists in efficacious photocatalytic decomposition and improves the efficacy.

Fig. S2 demonstrates the XRD analysis of $ZnO/(1\ wt\%)La_2O_3/NiO$, $ZnO/(3\ wt\%)La_2O_3/NiO$ and $ZnO/(5\ wt\%)La_2O_3/NiO$ samples. XRD patterns of the synthesized samples exhibited a series of characteristic reflections centered at 31.81°, 34.42°, 36.31°, 47.50°, 56.62°, 66.49°, 67.94°, and 69.09°, which can be respectively belonged to (1 0 0), (0 0 2), (1 0 1), (1 0 2), (1 1 0), (2 0 0), (1 1 2), and (2 0 1) planes. All these fingerprint reflections could be accredited to the ZnO-hexagonal phase (wurtzite structure) with space group of P63mc, which is very much in accordance with the reported value (JCPDS file number 36–1451) (Kumar et al., 2012). Additionally, the diffraction reflections situated at 37.23°, 43.22°, 62.88°, and 75.36° allocated to the (1 1 1), (2 0 0), (2 2 0), and (3 1 1) planes, correspondingly. These peaks are indexed to cubic NiO phase (JSPDS file number 65–2901) (Barzinjy et al., 2020). Eventually, the peak at 28.16° which is corresponding to (1 0 1) plane, confirms the existence of hexagonal La_2O_3 (JCPDS file number 05–0602) (Wang et al., 2014; Michel and Martinez-Preciado, 2015).

The FT-IR spectroscopy is commonly employed for detection the functional groups existent on the photocatalyst surface. The

FT-IR spectrum of ZnO/(3 wt%)La_2O_3/NiO heterostructure is demonstrated in Fig. S3. The wide-ranging peak situated at nearly 3438 cm^{-1} could be owing to stretching vibrations of (O–H) groups of physisorbed H_2O molecules. Besides, the absorption peak at approximately 1060 cm^{-1} corresponds to (C=O) stretching vibrations of acetate group. The characteristic peaks appeared at 580 cm^{-1} ascertained to the stretching vibration of the (Ni–O) bond (Biju et al., 2003). Ultimately, a peak centered at 864 cm^{-1} belonged to the (Zn–O) stretching vibrations (Shubha et al., 2020). The absorption peaks are noticed at approximately 665, 1020, and 1468 cm^{-1} could be associated with the stretching vibrations of the (La–O) bond (Xiao et al., 2014).

Morphological properties of the synthesized heterostructure i.e. ZnO/(3 wt%)La_2O_3/NiO are examined using FESEM analysis and the achievement of the nano-sized heterostructure is ascertained by TEM analysis, and the attained results are presented in Figs. S4 and S5, respectively. Lower magnification FESEM micrograph is demonstrated in Fig. S4a discloses that the ZnO/(3 wt%)La_2O_3/NiO is composed of clusters of particles and flakes. Fig. S4b & c is the higher magnification FESEM micrograph which displays the part of the sample is in the form of flakes in which all the flakes are interconnected and form a net-like structure with large pores. Based on the formerly published reports it can be supposed that the flake like morphology could be belonged to the NiO component of the heterostructure while the clusters could be the ZnO and La_2O_3 NPs in the heterostructure.

Morphology and size of the ZnO/(3 wt%)La_2O_3/NiO heterostructure are examined via HRTEM analysis at various magnifications as presented in Fig. S5. Fig. S5(a–c) illustrates the micrographs with varying magnifications which displays that the spherical particles are uniformly distributed throughout the sample with some incidents of aggregations could be noticed. The sizes of the particles are in the range of 10–15 nm. The selected area electron diffraction (SAED) pattern (Fig. S5d) shows the polycrystalline form of the material and the reflection planes obtained are consistent with the observations concluded from the XRD pattern.

The elemental analysis of the prepared ZnO/(3 wt%)La_2O_3/NiO heterostructure is scrutinized using EDX spectroscopy, as illustrated in Fig. S6. It discloses that the synthesized heterostructure contains the required elemental composition and the elements are well-dispersed throughout the composition, which could be play a synergetic role in improving the photo-catalytic efficacy. Furthermore, the EDX spectra of ZnO/(3 wt%)La_2O_3/NiO heterostructure, reveals that all the predicted elements like Zn, La, Ni, and O are existent and the percentage of elemental compositions are shown in the inset table, which is consistent with the stoichiometric amounts taken for preparation of the ZnO/(3 wt%) La_2O_3/NiO heterostructure.

3.2. Photocatalytic performance of ZnO/(X wt%)La_2O_3/NiO heterostructures

3.2.1. Influence of mole % of La_2O_3 doping

Three different samples of ZnO/La_2O_3/NiO with varying wt% of La_2O_3 (1 wt%, 3 wt% and 5 wt%) are prepared. Photocatalytic efficiency of all the samples are tested under identical experimental conditions (photocatalyst dose (15 mg), MB concentration (2 ppm) and pH (7) under visible light. The obtained results disclose that 3 wt% doping of La_2O_3 exhibits best degradation performance under the above-mentioned experimental conditions (Fig. 1). Therefore, all further optimization studies for the degradation is carried out with 3 wt% La_2O_3 supported ZnO/NiO nanoparticles.

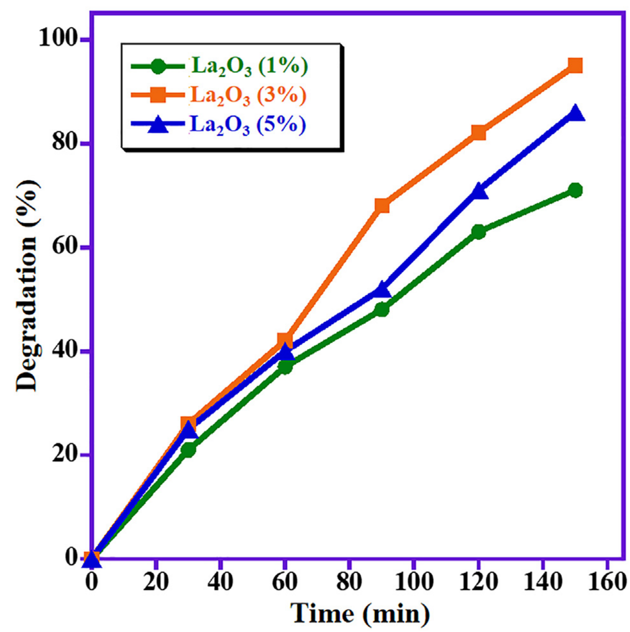

Fig. 1. Impact of weight percentage of 3 wt% La_2O_3 supported ZnO/NiO nanoparticles on MB photo-degradation.

3.2.2. Influence of light source

After the confirmation of the optimum % of La_2O_3 doping for the effective photo-catalytic efficacy of the synthesized heterostructures, efforts have been devoted to find out the proper light source that can give the best degradation performance of the as-synthesized heterostructure as the as-synthesized heterostructure is photolytically active in the UV region and visible region as assured from the UV–Vis spectrum. Therefore, the photo-catalytic decomposition of MB dye in presence of ZnO/(3 wt%)La_2O_3/NiO heterostructure is performed in three different environments i.e. dark, UV light irradiation, and natural solar irradiation. The obtained data showed that the prepared ZnO/(3 wt%)La_2O_3/NiO heterostructure is active in UV irradiation as well as in visible light, as realized by UV–Vis spectra obtained. When the degradation experiment conducted in the dark, the photo-degradation of the MB can be neglected. Furthermore, in case of the experiments carried out under visible irradiation and UV irradiation, the results revealed that the photodecomposition of MB under natural sunlight irradiation is extremely higher than the photo-degradation obtained in the UV light irradiation. For visible irradiation, the prepared ZnO/(3 wt%)La_2O_3/NiO heterostructure effectively degrade 95% of the MB dye than UV light irradiation which gave a degradation of 73% under the similar irradiation period (150 min). Based on that, it could be concluded that the ZnO/(3 wt%)La_2O_3/NiO heterostructure is effective photocatalyst under visible irradiation and the further optimization studies are performed under visible irradiation. The photocatalytic results obtained are plotted in Fig. 2.

3.2.3. Influence of amount of ZnO/(3 wt%)La_2O_3/NiO catalyst

After the confirmation of the photocatalyst composition and light source for the efficacious photocatalytic property of the synthesized ZnO/(3 wt%)La_2O_3/NiO heterostructure, the influence of photocatalyst dose on photodegradation of MB is also evaluated by carrying out various degradation experiments at varied amount of photocatalyst in the range of (5 mg–20 mg) under visible radiation (Fig. 3). The results obviously disclose that the photodecomposition of MB is considerably influenced by the photocatalyst dose. It is distinct that by increasing the photocatalyst dose from 5 mg to 15 mg, degradation of MB dye enhanced from 65% to 95%. This

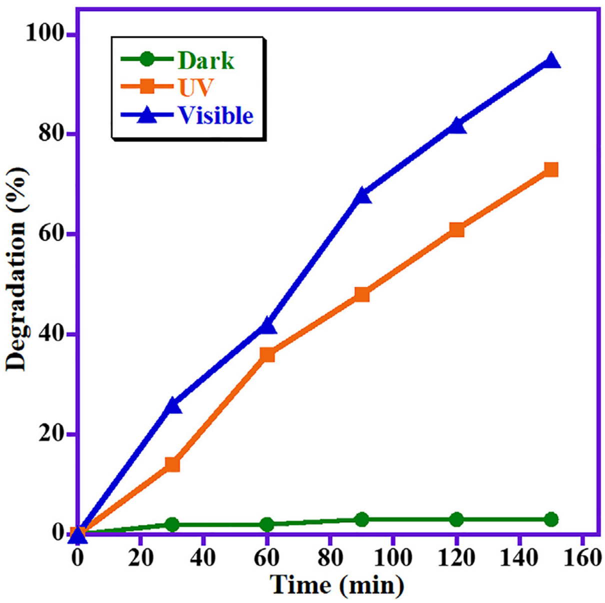

Fig. 2. Impact of light source on MB photo-degradation employing $ZnO/La_2O_3/NiO$ heterostructure.

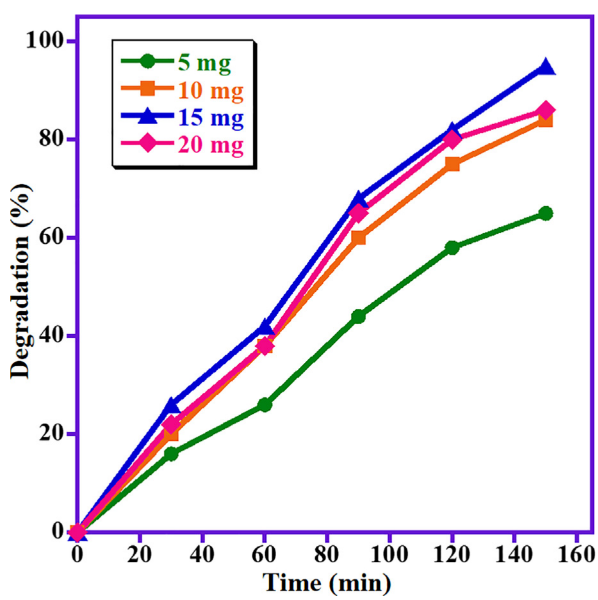

Fig. 3. Impact of photocatalyst dose on MB photo-degradation employing ZnO/(3 wt%)La_2O_3/NiO heterostructure.

enhancement in the degradation is attributed to the existence of more photocatalytic active sites in the medium that can generate more radicals by adding more amounts of ZnO/(3 wt%)La_2O_3/NiO photocatalyst. Nevertheless, further increase in the photocatalyst dose to 20 mg leads to a decrease in the degradation efficacy to 86% under the identical photocatalytic conditions. When the photocatalyst quantity exceeds a critical boundary there will not be sufficient space to disperse in the solution and the particles can stick to each other and become aggregated, owing to the particles surface energy. Hence, the photocatalytic active sites are blocked or covered-up and the degradation efficacy of the system decreases (Nezam et al., 2016). Hence, 15 mg is selected as the optimal photocatalyst amount and is utilized for the rest of experiments to optimize other parameters. The obtained data is graphically illustrated in Fig. 3.

3.2.4. Influence of concentration of MB

The impact of initial dye concentrations on the decomposition performance of the MB is also assessed by varying the concentration of MB from 2 ppm to 15 ppm under visible irradiation while maintaining the photocatalyst dose of 15 mg constant. The attained photocatalytic data is graphically presented in Fig. 4. The obtained results disclosed that the performance of the ZnO/(3 wt%)La_2O_3/NiO photocatalyst is inversely proportional to the dye concentration at the similar conditions, i.e. maximum degradation efficacy is observed at lowest MB concentration (2 ppm). By raising the MB concentration from 2 ppm to 15 ppm, the degradation activity of MB gradually declined from 97% to 70%. This presumably owing to the decreased absorption of light on the photocatalyst surface by raising the dye concentration, which in-turn reduces the production of $OH^{\cdot}$ radicals which play a vital role in the photodegradation process. So, it is indispensable to increase the photocatalyst quantity as the concentration of dye increases. As a result, the highest degradation performance is achieved at the MB dye concentration of 2 ppm.

3.2.5. Influence of pH value

It is well known that pH of the solution is one of the most significant parameters in the photo-catalytic degradation of organic dyes attributed to the change in surface charge of photocatalyst, which in-turn has a considerable effect on the photo-catalytic efficiency. Usually, the photo-catalytic performance of the photocatalyst directly related to availability of $OH^{\cdot}$ radicals in the reaction medium, which improves the photo-catalytic decomposition of MB dye many folds in alkaline aqueous solution. Fig. 5 displayed the impact of pH value on photo-degradation of MB dye in presence of ZnO/(3 wt%)La_2O_3/NiO photocatalyst. The impact of pH value on the removal of MB is also examined at three different pH values of 4, 7, and 10. The results illustrated that by raising the pH value to 10, higher photodegradation is achieved. At lowest pH value (i.e., pH 4), the lowest degradation performance is obtained with 52% degradation of MB. As expected, when the pH of the solution is increased, the ZnO/(3 wt%)La_2O_3/NiO photocata-

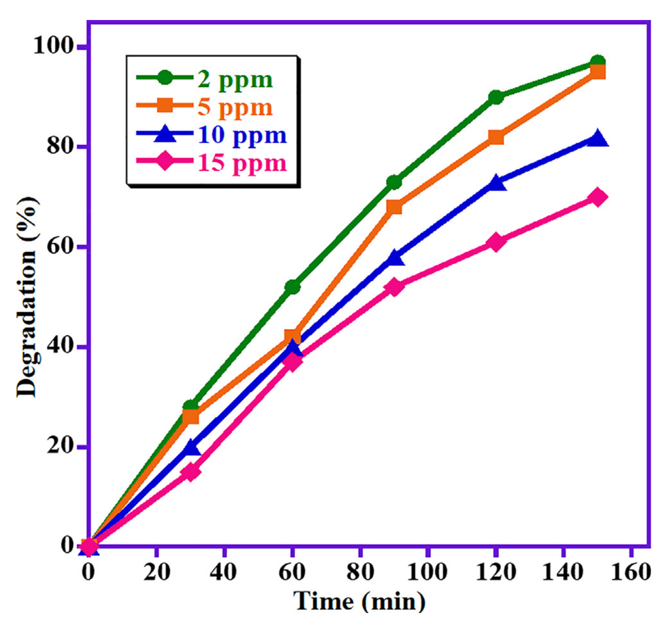

Fig. 4. Impact of MB concentration on the catalytic performance of ZnO/(3 wt%)La_2O_3/NiO heterostructure on the MB photo-degradation.

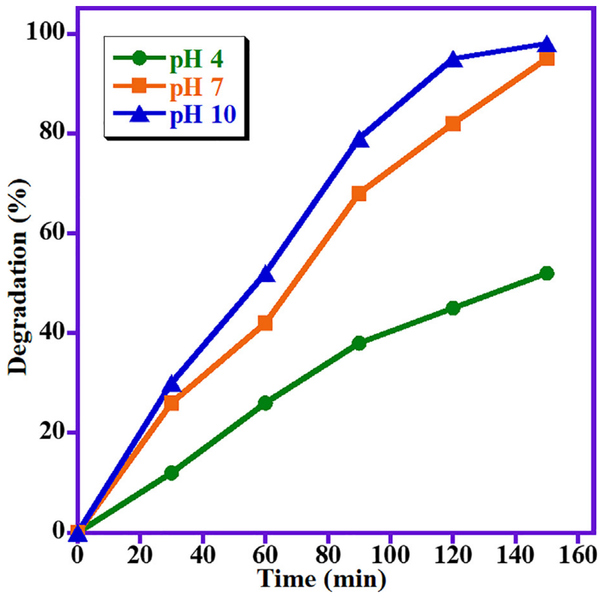

Fig. 5. Impact of pH value on the catalytic performance of ZnO/(3 wt%)La_2O_3/NiO on the MB photo-degradation.

lyst showed maximum degradation activity and approximately 98% degradation of MB has achieved for pH 10. This is possibly because of the higher pH value which leads to formation of negative charges on the surface as well as MB is a cationic dye that possesses a positive charge. Hence, higher amounts of OH· radicals are adsorbed on the photocatalyst surface and the photo-degradation process is performed more efficiently in higher pH values (Motlagh et al., 2015). Fig. 6 illustrates that the photocatalytic decomposition reactions for various pH values at optimum reaction circumstances followed a pseudo-1st-order reaction kinetics which is given by Eq. (2) as:

$$\ln = kt \quad (2)$$

where C_0 and C_t are the initial dye concentration and final dye concentration at time t, correspondingly, and k is the first-order rate constant. The obtained degradation rate constants (k) are 0.0151 min^{-1}, 0.0427 min^{-1}, and 0.0621 min^{-1} for the pH values of 4, 7, and 10, respectively.

3.3. Photoluminescence study

Indeed, the hydroxyl (OH·) radicals are extremely reactive and non-stable chemical species and had a significant impact in the photo-catalytic decomposition of industrial dye molecules. To find out whether the OH· radicals are being formed by the prepared photocatalyst i.e., ZnO/(3 wt%)La_2O_3/NiO, coumarin has been chosen as a substrate model, which is a sensitive and simple technique for detection of the OH· free radicals. In the presence of OH· radicals produced through ZnO/(3 wt%)La_2O_3/NiO catalyst, coumarin transforms to 7-hydroxy-coumarin which is a luminous compound shows a photoluminescent (PL) peak at λ = 455 nm. In this investigation, 0.1 g of the ZnO/(3 wt%)La_2O_3/NiO photocatalyst is added to the 50 mL of coumarin solution with concentration of 0.001 M under natural solar irradiation. At passing 10 min, 2 mL of the sample is injected to the PL instrument, which showed that the existence of PL peak at λ = 455 nm (Fig. 7), confirming that the production of OH· radicals, an essential chemical species for the photo-degradation of dye molecules (Nagaraju et al., 2017). Consequently, it can be stated that the photodecomposition of MB dye occurs through a free-radical mechanism over the prepared ZnO/(3 wt%)La_2O_3/NiO photocatalyst.

A comparison of outstanding photo-catalytic degradation efficacy of the ZnO/(3 wt%)La_2O_3/NiO photocatalyst for photodecomposition of MB with formerly reported ZnO-based photo-catalytic systems, as compiled in Table 1. It is distinctly noticed that ternary the ZnO/(3 wt%)La_2O_3/NiO photocatalyst in the current study exhibits superior photo-degradation efficiency.

3.4. Photocatalytic mechanism

The photocatalytic degradation mechanism is suggested and schematically presented in Scheme 2, illustrating transfer and participation of photo-produced electrons in the conduction band (CB) of semiconductor La_2O_3 NPs and their involvement in the reduction reactions under natural solar radiation.

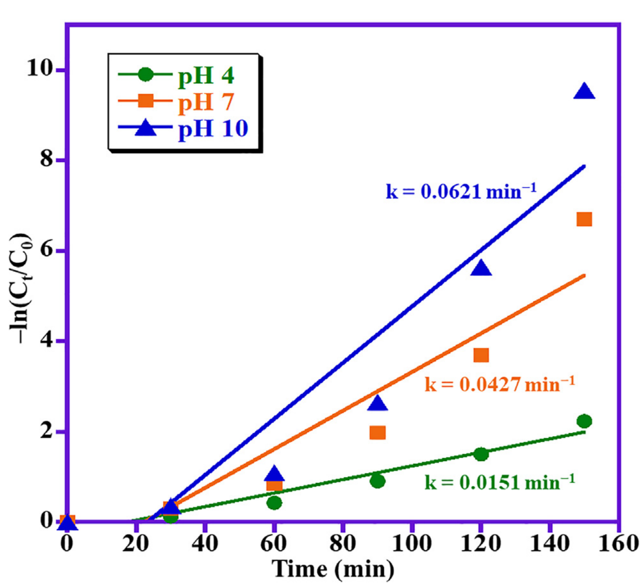

Fig. 6. Psuedo-first-order kinetics for MB photo-degradation over ZnO/(3 wt%) La_2O_3/NiO photocatalyst.

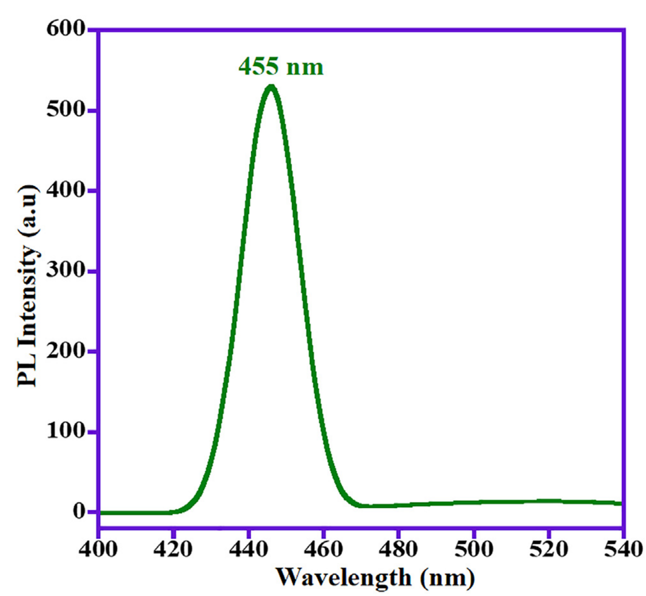

Fig. 7. PL spectrum indicating production of OH· radicals via ZnO/(3 wt%)La_2O_3/NiO photocatalyst.

Table 1
Comparison of photo-catalytic efficacy of $ZnO/(3\ wt\%)La_2O_3/NiO$ for MB decomposition with previously reported analogous photo-catalysts containing ZnO NPs.

Catalyst	MB conc.	Photocatalyst dose	Light source	t. (min)	Degradation (%)	Ref.
$ZnO/(3\ wt\%)La_2O_3/NiO$	2 ppm	15 mg	Sunlight	150	98	Herein
NiO–ZnO–Ag	10 ppm	20 mg	UV lamp	90	94	(Aydoghmish, Hassanzadeh-Tabrizi, and Saffar-Teluri, 2019)
$ZnO-SiO_2$	9 ppm	10 mg	Sunlight	90	97.8	(Stanley, 2019)
ZnO/PAN	10 ppm	50 mg	Sunlight	450	99.2	(Zhou et al., 2018)
ZnO NWs	10 ppm	100 mg/L	Sunlight	4320	100	(Mahana et al., 2020)
ZnO/GRO	25 ppm	100 mg	Sunlight	105	86.9	(Zarrabi, Haghighi, and Alizadeh, 2018)
N/La–ZnO	15 ppm	50 mg	Sunlight	60	97	(Youssef and Yakout, 2020)
TiO_2-ZnO/rGO	0.3 ppm	0.1 g/L	300 W Xe-lamp	120	92	(Wang et al., 2016)
ZnO–Cu	0.03 mM	5 mg	10 W UV-lamp	180	60	(Shah et al., 2020)
ZnO-supported MnO	100 ppm	40 mg	15 W UV-lamp	120	95	(Siddique, Fayaz, and Saeed, 2020)
1.5%Nd-Gd-ZnO	20 mg/L	100 mg/L	300 W Vis. light	120	93	(Akhtar et al., 2020)
Ce-Ag-ZnO/Fe_3O_4	10 ppm	30 mg	15 W UV lamp	100	99	(Heshmatpour and Abdikhani, 2019)
Cu_2O–ZnO	2 ppm	0.4 g/L	100 W W-lamp	60	78	(Norouzi et al., 2021)
TiO_2/ZnO/rGO	0.3 ppm	0.1 g/L	300 W Xe-lamp	120	92	(Raghavan, Thangavel, and Venugopal, 2015)
RGO-Ag/ZnO	10 ppm	50 mg	UV lamp	120	99	(Belachew et al., 2020)
WO_3/ZnO@rGO	5 ppm	10 mg	200 W Vis. light	90	94.1	(Chaudhary et al., 2020)
ZnO/Cu/rGO	10^{-5} M	25 mg	300 W Xe-lamp	60	97	(Asgharian et al., 2019)
GaN-ZnO/g-C_3N_4	50 ppm	100 mg	75 W Vis. light	300	98.1	(Van et al., 2020)
Ag-ZnO	40 ppm	400 mg/L	Vis. light	120	96.2	(Satdeve, Ugwekar, and Bhanvase, 2019)

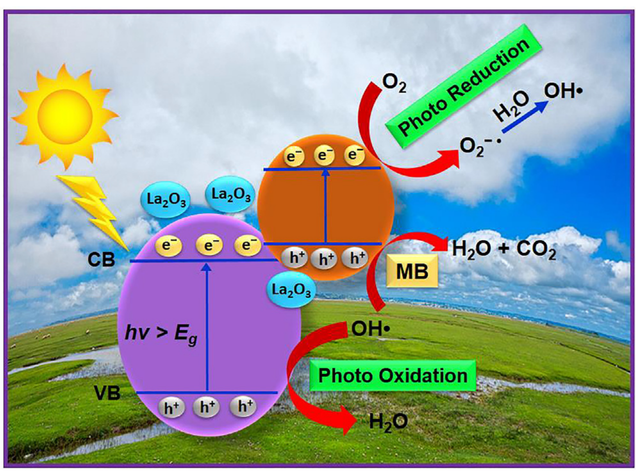

Scheme 2. Scheme depiction of degradation methodology of MB.

4. Conclusions

In summing up, we have efficiently fabricated heterojunction $ZnO/(X\ wt\%)La_2O_3/NiO$ photocatalysts with different percentages of La_2O_3 as a dopant via an eco-friendly and facile combustion method. The characterization of the as-synthesized material reveals the crystalline nature and nano-sized $ZnO/(3\ wt\%)La_2O_3/$ NiO heterostructure with 3 wt% La_2O_3 . The photo-degradation reactivity of the synthesized $ZnO/(3\ wt\%)La_2O_3/NiO$ nanocomposites has been assessed via the photo-decomposition of MB dye as a benchmark reaction under natural sunlight irradiation. Results of MB degradation disclosed that the as-fabricated photocatalyst is highly effective and the degradation performance is considerably influenced by the variations in light source, catalyst loading, catalyst dose, MB concentration, irradiation time and pH of solution and the kinetics of the photocatalyst showed that 98% degradation in 150 mins under the optimal experimental conditions. Hence, further studies into the kinetics and fine-tuning of the economic and eco-friendly catalyst is in progress and will be reported in future. Hence, further investigations into the kinetics and fine-tuning of the environmental-friendly and economic catalyst is in progress and shall be reported in future. Eventually, the results demonstrated that the $ZnO/(3\ wt\%)La_2O_3/NiO$ nanocomposite has found to be an efficacious photocatalyst for the photo-decomposition of MB under natural sunlight radiation without any harmful impact on the environment.

Declaration of Competing Interest

The authors declare that they have no known competing financial interests or personal relationships that could have appeared to influence the work reported in this paper.

Acknowledgements

The authors would like to acknowledge the Researchers supporting project number (RSP-2021/222), King Saud University, Riyadh, Saudi Arabia. This work was supported by Vision Group on Science and Technology (SMYSR-2016; GRD 506) Govt. of Karnataka, India, Authors are thankful to Principal and Management of Don Bosco Institute of Technology for their constant support and Technical Research Centre–Microscopy lab at JNCASR for providing microscopy facilities.

Appendix A. Supplementary data

Supplementary data to this article can be found online at https://doi.org/10.1016/j.jksus.2021.101738.

References

Akhtar, J., Tahir, M.B., Sagir, M., Bamufleh, H.S., 2020. Improved photocatalytic performance of Gd and Nd co-doped ZnO nanorods for the degradation of methylene blue. Ceram. Int. 46 (8), 11955–11961.

Alharthi, Fahad A., Nabil Al-Zaqri, Adel El marghany, Abdulaziz Ali Alghamdi, Ali Q. Alorabi, Neazar Baghdadi, H. S. Al-Shehri, Rizwan Wahab, and Naushad Ahmad. 2020. 'Synthesis of nanocauliflower ZnO photocatalyst by potato waste and its photocatalytic efficiency against dye', *J. Mater. Sci.: Mater. Electron.*, 31: 11538-47.

Asgharian, Maedeh, Mehdipourghazi, Mohsen, Khoshandam, Behnam, Keramati, Narjes, 2019. Photocatalytic degradation of methylene blue with synthesized rGO/ZnO/Cu. Chem. Phys. Lett. 719, 1–7.

Atla, Shashi B, Lin, Wun-Rong, Chien, Ting-Che, Tseng, Min-Jen, Shu, Jwu-Ching, Chen, Chien-Cheng, Chen, Chien-Yen, 2018. Fabrication of Fe3O4/ZnO magnetite core shell and its application in photocatalysis using sunlight. Mater. Chem. Phys. 216, 380–386.

Aydoghmish, Samireh Mohammadi, Hassanzadeh-Tabrizi, S.A., Saffar-Teluri, A., 2019. Facile synthesis and investigation of NiO–ZnO–Ag nanocomposites as efficient photocatalysts for degradation of methylene blue dye. Ceram. Int. 45, 14934–14942.

Azam, Mohammad, Al-Resayes, Sa.ud.I., Wabaidur, Saikh Mohammad, Trzesowska-Kruszynska, Agata, Kruszynski, Rafal, Mohapatra, Ranjan K, Mohammed Rafiq, H., Siddiqui, 2018. Cd (II) complex constructed from dipyridyl imine ligand: Design, synthesis and exploration of its photocatalytic degradation properties. Inorg. Chim. Acta 471, 698–704.

Barzinjy, A.A., Hamad, S.M., Aydin, S., Ahmed, M.H., Hussain, F.H.S., 2020. Green and eco-friendly synthesis of Nickel oxide nanoparticles and its photocatalytic activity for methyl orange degradation. J. Mater. Sci.: Mater. Electron. 31, 11303–11316.

Belachew, Neway, Kahsay, Mebrahtu Hagos, Tadesse, Aschalew, Basavaiah, Keloth, 2020. 'Green synthesis of reduced graphene oxide grafted Ag/ZnO for photocatalytic abatement of methylene blue and antibacterial activities. J. Environ. Chem. Eng. 8 (5), 104106. https://doi.org/10.1016/j.jece:2020.104106.

Bharathi, P., Harish, S., Archana, J., Navaneethan, M., Ponnusamy, S., Muthamizhchelvan, C., Shimomura, M., Hayakawa, Y., 2019. Enhanced charge transfer and separation of hierarchical CuO/ZnO composites: The synergistic effect of photocatalysis for the mineralization of organic pollutant in water. Appl. Surf. Sci. 484, 884–891.

Biju, V., Abdul, M., Khadar, 2003. Fourier transform infrared spectroscopy study of nanostructured nickel oxide. Spectrochim. Acta Part A Mol. Biomol. Spectrosc. 59, 121–134.

Chaudhary, Khadija, Shaheen, Nusrat, Zulfiqar, Sonia, Sarwar, Muhammad Ilyas, Suleman, Muhammad, Agboola, Philips O, Shakir, Imran, Warsi, Muhammad Farooq, 2020. Binary WO3-ZnO nanostructures supported rGO ternary nanocomposite for visible light driven photocatalytic degradation of methylene blue. Synth. Met. 269, 116526.

Chaudhary, Savita, Kaur, Yesbinder, Jayee, Bhumika, Chaudhary, Ganga Ram, Umar, Ahmad, 2018. NiO nanodisks: Highly efficient visible-light driven photocatalyst, potential scaffold for seed germination of Vigna Radiata and antibacterial properties. J. Cleaner Prod. 190, 563–576.

Dutta, Amit Kumar, Maji, Swarup Kumar, Adhikary, Bibhutosh, 2014. γ-Fe2O3 nanoparticles: An easily recoverable effective photo-catalyst for the degradation of rose bengal and methylene blue dyes in the waste-water treatment plant. Mater. Res. Bull. 49, 28–34.

El-Barasi, Najla M, Miloud, Miloud M, El-ajaily, Marei M, Mohapatra, Ranjan K, Sarangi, Ashish K, Das, Debadutta, Mahal, Ahmed, Parhi, Pankaj K, Pintilie, Lucia, Barik, Soumya R, 2020. Synthesis, structural investigations and antimicrobial studies of hydrazone based ternary complexes with Cr (III), Fe (III) and La (III) ions. J. Saudi Chem. Soc. 24, 492–503.

Feng, Yimeng, Wang, Yazi, Li, Mingyang, Lv, Shasha, Li, Wei, Li, Zhengcao, 2018. Novel visible light induced Ag2S/g-C3N4/ZnO nanoarrays heterojunction for efficient photocatalytic performance. Appl. Surf. Sci. 462, 896–903.

Gonte, Renuka, Balasubramanian, K., 2016. Heavy and toxic metal uptake by mesoporous hypercrosslinked SMA beads: isotherms and kinetics. J. Saudi Chem. Soc. 20, S579–S590.

He, Y.P., Miao, Y.M., Li, C.R., Wang, S.Q., Cao, L., Xie, S.S., Yang, G.Z., Zou, B.S., Burda, C., 2005. Size and structure effect on optical transitions of iron oxide nanocrystals. Phys. Rev. B 71, 125411.

Hernández-Carrillo, M.A., Torres-Ricárdez, R., García-Mendoza, M.F., Ramírez-Morales, E., Rojas-Blanco, L., Díaz-Flores, L.L., Sepúlveda-Palacios, G.E., Paraguay-Delgado, F., Pérez-Hernández, G., 2018. Eu-modified ZnO nanoparticles for applications in photocatalysis. Catal. Today.

Heshmatpour, Felora, Abdikhani, Marzieh Sadat, 2019. Ce-Ag-ZnO/Fe3O4 nanocomposites: A novel magnetically separable photocatalyst for highly efficient photodegradation of contaminants. Physica B 570, 312–319.

Koutavarapu, Ravindranadh, Bathula Babu, Ch., Reddy, Venkata, Yoo, Kisoo, Cho, Migyung, Shim, Jaesool, 2020. A novel one-pot approach of ZnWO 4 nanorods decorated onto gC 3 N 4 nanosheets: 1D/2D heterojunction for enhanced solar-light-driven photocatalytic activity. J. Mater. Sci. 55, 1170–1183.

Kumar, Pushpendra, Singh, Jai, Parashar, Vyom, Kedar Singh, R.S., Tiwari, ON Srivastava, Ramam, Koduri, Pandey, Avinash C, 2012. Investigations on structural, optical and second harmonic generation in solvothermally synthesized pure and Cr-doped ZnO nanoparticles. CrystEngComm 14, 1653–1658.

Li, Wei, Wang, Guojing, Chen, Chienhua, Liao, Jiecui, Li, Zhengcao, 2017. Enhanced visible light photocatalytic activity of ZnO nanowires doped with Mn2+ and Co2+ ions. Nanomaterials 7, 20.

Liu, Yanli, Li, Guizhi, Mi, Riding, Deng, Congkun, Gao, Pengzhao, 2014. An environment-benign method for the synthesis of p-NiO/n-ZnO heterostructure with excellent performance for gas sensing and photocatalysis. Sens. Actuators, B 191, 537–544.

López, Uribe, Alvarez Lemus, MC Hidalgo, R López González, P Quintana Owen, S Oros-Ruiz, SA Uribe López, and J Acosta. 2019. 'Synthesis and characterization of ZnO-ZrO2 nanocomposites for photocatalytic degradation and mineralization of phenol', *J. Nanomater.*, 2019.

Mahana, Abhijeet, Guliy, Olga I., Momin, Sengjrang Ch, Lalmuanzeli, Ruthi, Mehta, Surya Kant, 2020. Sunlight-driven photocatalytic degradation of methylene blue using ZnO nanowires prepared through ultrasonication-assisted biological process using aqueous extract of Anabaena doliolum. Opt. Mater. 108, 110205. https://doi.org/10.1016/j.optmat.2020.110205.

Martínez-Vargas, Blanca L, Cruz-Ramírez, Marisela, Díaz-Real, Jesús A, Rodríguez-López, J.L., Bacame-Valenzuela, Francisco Javier, Ortega-Borges, Raúl, Reyes-Vidal, Yolanda, Ortiz-Frade, Luis, 2019. Synthesis and characterization of n-ZnO/p-MnO nanocomposites for the photocatalytic degradation of anthracene. J. Photochem. Photobiol., A 369, 85–96.

Maruthupandy, Muthuchamy, Qin, Pan, Muneeswaran, Thillaichidambaram, Rajivgandhi, Govindan, Quero, Franck, Song, Ji-Ming, 2020. Graphene-zinc oxide nanocomposites (G-ZnO NCs): Synthesis, characterization and their photocatalytic degradation of dye molecules. Mater. Sci. Eng., B 254, 114516.

Michel, Carlos R, Martinez-Preciado, Alma H, 2015. CO sensing properties of novel nanostructured La2O3 microspheres. Sens. Actuators, B 208, 355–362.

Motlagh, Mahboube Mohaghegh, Hassanzadeh-Tabrizi, S.A., Saffar-Teluri, Ali, 2015. Sol–gel synthesis of Mn 2 O 3/Al 2 O 3/SiO 2 hybrid nanocomposite and application for removal of organic dye. J. Sol-Gel Sci. Technol. 73, 9–13.

Nagaraju, G., Nagabhushana, H., Suresh, D., Anupama, C., Raghu, G.K., Sharma, S.C., 2017. Vitis labruska skin extract assisted green synthesis of ZnO super structures for multifunctional applications. Ceram. Int. 43, 11656–11667.

Natarajan, Thillai Sivakumar, Thampi, K. Ravindranathan, Tayade, Rajesh J., 2018. Visible light driven redox-mediator-free dual semiconductor photocatalytic systems for pollutant degradation and the ambiguity in applying Z-scheme concept. Appl. Catal. B 227, 296–311.

Nezam, Amene, Saffar-Teluri, A., Hassanzadeh-Tabrizi, S.A., 2016. The high efficiency of Al 2 O 3–SiO 2–CuO nanocomposites as an adsorbent: synthesis and dye removal efficiency. Res. Chem. Intermed. 42, 4999–5011.

Norouzi, Abbas, Nezamzadeh-Ejhieh, Alireza, Fazaeli, Razieh, 2021. A Copper(I) oxide-zinc oxide nano-catalyst hybrid: Brief characterization and study of the kinetic of its photodegradation and photomineralization activities toward methylene blue. Mater. Sci. Semicond. Process. 122, 105495. https://doi.org/10.1016/j.mssp.2020.105495.

Pirkarami, Azam, Olya, Mohammad Ebrahim, 2017. Removal of dye from industrial wastewater with an emphasis on improving economic efficiency and degradation mechanism. J. Saudi Chem. Soc. 21, S179–S186.

Pirmoradi, Mysam, Hashemian, Saeedeh, Shayesteh, Mohammad Reza, 2017. Kinetics and thermodynamics of cyanide removal by ZnO@ NiO nanocrystals. Trans. Nonferrous Metals Soc. China 27, 1394–1403.

Raghavan, Nivea, Thangavel, Sakthivel, Venugopal, Gunasekaran, 2015. Enhanced photocatalytic degradation of methylene blue by reduced graphene-oxide/titanium dioxide/zinc oxide ternary nanocomposites. Mater. Sci. Semicond. Process. 30, 321–329.

Saravanakumar, K., Muthuraj, V., Vadivel, S., 2016. Constructing novel Ag nanoparticles anchored on MnO 2 nanowires as an efficient visible light driven photocatalyst. RSC Adv. 6, 61357–61366.

Satdeve, N.S., Ugwekar, R.P., Bhanvase, B.A., 2019. Ultrasound assisted preparation and characterization of Ag supported on ZnO nanoparticles for visible light degradation of methylene blue dye. J. Mol. Liq. 291, 111313.

Senobari, Samaneh, Nezamzadeh-Ejhieh, Alireza, 2018. A comprehensive study on the enhanced photocatalytic activity of CuO-NiO nanoparticles: designing the experiments. J. Mol. Liq. 261, 208–217.

Shah, Aqeel Ahmed, Bhatti, Muhammad Ali, Tahira, Aneela, Chandio, Ali Dad, Channa, Iftikhar A, Sahito, Ali Ghulam, Chalangar, Ebrahim, Willander, Magnus, Nur, Omer, Ibupoto, Zafar Hussain, 2020. Facile synthesis of copper doped ZnO nanorods for the efficient photo degradation of methylene blue and methyl orange. Ceram. Int. 46, 9997–10005.

Shubha, J. Pranesh, Adil, Syed F., Khan, Mujeeb, Hatshan, Mohammad R., Khan, Aslam, 2021. Facile Fabrication of a ZnO/Eu2O3/NiO-Based Ternary Heterostructure Nanophotocatalyst and Its Application for the Degradation of Methylene Blue. ACS Omega 6 (5), 3866–3874.

Shubha, Jayachamarajapura, Pranesh, Lanka, Diwya, 2020. Green synthesis of ZnO/Dy/NiO heterostructures for enhanced photocatalytic applications. J. Photocatal. 1, 30–36.

Siddique, Mohsin, Fayaz, Naila, Saeed, Muhammad, 2020. Synthesis, characterization, photocatalytic activity and gas sensing properties of zinc doped manganese oxide nanoparticles. Physica B 412504.

Stanley, R., 2019. Enhanced sunlight photocatalytic degradation of methylene blue by rod-like ZnO-SiO2 nanocomposite. Optik 180, 134–143.

Tahir, Muhammad Nawaz, 2020. Synthesis of hierarchically organized α-Fe 2 O 3 nanostructures for the photocatalytic degradation of methylene blue. Emergent Mater. 3, 605–612.

Tahir, Muhammad Nawaz, 2021. Non-aqueous synthesis of AuCu@ ZnO alloy-semiconductor heteroparticles for photocatalytical degradation of organic dyes. J. Saudi Chem. Soc. 25, 101210.

Tahir, Muhammad Nawaz, Natalio, Filipe, Cambaz, Musa Ali, Panthöfer, Martin, Branscheid, Robert, Kolb, Ute, Tremel, Wolfgang, 2013. Controlled synthesis of linear and branched Au@ ZnO hybrid nanocrystals and their photocatalytic properties. Nanoscale 5, 9944–9949.

Tang, Chunmei, Chen, Ch.u., Zhang, Hongyan, Zhang, Jun, Li, Zhijun, 2020. Enhancement of degradation for nitrogen doped zinc oxide to degrade methylene blue. Physica B 583, 412029.

Van, Kim Nguyen, Viet Nga Nguyen Thi, Thu Phuong Tran Thi, Thanh Tam Truong, Thanh Lieu Le Thi, Ha Tran Huu, and Vien Vo. 2020. 'A novel preparation of GaN-ZnO/g-C3N4 photocatalyst for methylene blue degradation', Chem. Phys. Lett. 138191.

Wang, Fangzhi, Li, Wenjun, Gu, Shaonan, Li, Hongda, Liu, Xintong, Wang, Mingzhu, 2016a. Fabrication of $FeWO_4$@$ZnWO_4$/ZnO heterojunction photocatalyst: synergistic effect of $ZnWO_4$/ZnO and $FeWO_4$@$ZnWO_4$/ZnO heterojunction structure on the enhancement of visible-light photocatalytic activity. ACS Sustainable Chem. Eng. 4 (12), 6288–6298.

Wang, Kunjie, Yanping, Wu., Li, Hongxia, Li, Mingliang, Guan, Feng, Fan, Haiyan, 2014. A hybrid antioxidizing and antibacterial material based on Ag–La2O3 nanocomposites. J. Inorg. Biochem. 141, 36–42.

Wang, Longfei, Liu, Shuhai, Wang, Zheng, Zhou, Yongli, Qin, Yong, Wang, Zhong Lin, 2016b. Piezotronic effect enhanced photocatalysis in strained anisotropic ZnO/TiO2 nanoplatelets via thermal stress. ACS Nano 10, 2636–2643.

Xiao, Yanfei, Feng, Zongyu, Huang, Xiaowei, Huang, Li, Long, Zhiqi, Wang, Qiang, Hou, Yongke, 2014. Synthesis of lanthanum oxide nanosheets by a green carbonation process. Chin. Sci. Bull. 59, 1864–1867.
Youssef, A.M., Yakout, S.M., 2020. Superior sunlight photocatalytic of N/La codoped ZnO nanostructures synthesized using different chelating agents. Opt. Mater. 107, 110072.
Zarrabi, Mahdi, Haghighi, Mohammad, Alizadeh, Reza, 2018. Sonoprecipitation dispersion of ZnO nanoparticles over graphene oxide used in photocatalytic degradation of methylene blue in aqueous solution: influence of irradiation time and power. Ultrason. Sonochem. 48, 370–382.
Zhang, Yu., Cui, Wenquan, An, Weijia, Liu, Li, Liang, Yinghua, Zhu, Yongfa, 2018a. Combination of photoelectrocatalysis and adsorption for removal of bisphenol A over TiO2-graphene hydrogel with 3D network structure. Appl. Catal. B 221, 36–46.
Zhang, Zewu, Ma, Yuhang, Xiaohai, Bu., Qiong, Wu., Hang, Zusheng, Dong, Zhao, Xiaohan, Wu., 2018b. Facile one-step synthesis of TiO 2/Ag/SnO 2 ternary heterostructures with enhanced visible light photocatalytic activity. Sci. Rep. 8, 1–11.
Zhao, Si-Wei, Zuo, Hong-Fen, Guo, Yuan-Ru, Pan, Qing-Jiang, 2017. Carbon-doped ZnO aided by carboxymethyl cellulose: fabrication, photoluminescence and photocatalytic applications. J. Alloy. Compd. 695, 1029–1037.
Zhou, Ying, Hou-Yong, Yu., Ji-Ping, Gu., Zhu, Jia-Ying, Zhu, Mai-Hao, Guan, Ying, Yao, Ju-Ming, 2018. Novel fabrication of modulated carpenterworm-like zinc oxide/polyacrylonitrile composite nanofibers for photocatalytic degradation of methylene blue dye. J. Taiwan Inst. Chem. Eng. 91, 548–555.